Journal of Physics: Conference Series **675** (2016) 032001 doi:10.1088/1742-6596/675/3/032001

H, He, Li and Be Isotopes in the PAMELA-Experiment

W Menn[19], O Adriani[5,6], G C Barbarino[7,8], G A Bazilevskaya[9], R Bellotti[10,11], M Boezio[2], E A Bogomolov[12], M Bongi[4,6], V Bonvicini[2], S Bottai[6], A Bruno[10,11], F Cafagna[11], D Campana[8], P Carlson[13], M Casolino[3,15], G Castellini[16], C De Donato[3], C De Santis[14], N De Simone[3], V di Felice [3,4] V Formato[1,2], A M Galper[17], A V Karelin[17], S V Koldashov[17], S Koldobskiy[17], S Y Krutkov[12], A N Kvashnin[9], A Leonov[17], V Malakhov[17], L Marcelli[14], M Martucci[14,18], A G Mayorov[17], M Merge'[3,14], V V Mikhailov[17], E Mocchiutti[2], A Monaco[10,11], N Mori[6], R Munini[1,2], G Osteria[8], F Palma[3,14], B Panico[8], P Papini[6], M Pearce[13], P Picozza[3,14], M Ricci[18], S B Ricciarini[16], R Sarkar[2], V Scotti[7,8], M Simon[19], R Sparvoli[3,14], P Spillantini[5,6], Y I Stozhkov[9], A Vacchi[2], E Vannuccini[6], G Vasilyev[12], S A Voronov[17], Y T Yurkin[17], G Zampa[2], N Zampa[2], M S Potgieter [21] and E E Vos [21]

[1] University of Trieste, Department of Physics, I-34147 Trieste, Italy
[2] INFN, Sezione di Trieste I-34149 Trieste, Italy
[3] INFN, Sezione di Rome "Tor Vergata", I-00133 Rome, Italy
[4] Agenzia Spaziale Italiana (ASI) Science Data Center, I-00044 Frascati, Italy
[5] University of Florence, Department of Physics, I-50019 Sesto Fiorentino, Florence, Italy
[6] INFN, Sezione di Florence, I-50019 Sesto Fiorentino, Florence, Italy
[7] University of Naples "Federico II", Department of Physics, I-80126 Naples, Italy
[8] INFN, Sezione di Naples, I-80126 Naples, Italy
[9] Lebedev Physical Institute, RU-119991, Moscow, Russia
[10] University of Bari, Department of Physics, I-70126 Bari, Italy
[11] INFN, Sezione di Bari, I-70126 Bari, Italy
[12] Ioffe Physical Technical Institute, RU-194021 St. Petersburg, Russia
[13] KTH, Department of Physics, and the Oskar Klein Centre for Cosmoparticle Physics, AlbaNova University Centre, SE-10691 Stockholm, Sweden
[14] University of Rome "Tor Vergata", Department of Physics, I-00133 Rome, Italy
[15] RIKEN, Advanced Science Institute, Wako-shi, Saitama, Japan
[16] IFAC, I-50019 Sesto Fiorentino, Florence, Italy
[17] National Research Nuclear University MEPhI (Moscow Engineering Physics Institute), Kashirskoe highway 31, Moscow, 115409, Russia
[18] INFN, Laboratori Nazionali di Frascati, Via Enrico Fermi 40, I-00044 Frascati, Italy
[19] Universität Siegen, Department of Physics, D-57068 Siegen, Germany
[20] INFN, Sezione di Perugia, I-06123 Perugia, Italy

E-mail: menn@pamela.physik.uni-siegen.de

Abstract. On the 15th of June 2006, the PAMELA satellite-borne experiment was launched from the Baikonur cosmodrome and it has been collecting data since July 2006. The apparatus comprises a time-of-flight system, a silicon-microstrip magnetic spectrometer, a silicon-tungsten electromagnetic calorimeter, an anti-coincidence system, a shower tail counter scintillator and

a neutron detector. The scientific objectives addressed by the mission are the measurement of the antiprotons and positrons spectra in cosmic rays, the hunt for antinuclei as well as the determination of light nuclei fluxes from hydrogen to oxygen in a wide energy range and with very high statistics. In this paper the identification capability for light nuclei isotopes using two different detector systems (Time-of-Flight and multiple dE/dx measurements in the calorimeter) and preliminary results of the isotopic ratios will be presented.

1. Introduction

Measurements of the isotopic composition of elements of the cosmic radiation provide significant constraints on cosmic ray source composition and cosmic ray transport and acceleration in the galaxy. The isotopes of Li, Be, and B in cosmic rays are pure spallation products of primary cosmic rays, mainly C, N, and O, when they interact with interstellar matter during their propagation in the Galaxy. The rare isotopes ^{2}H and ^{3}He in cosmic rays are believed to originate mainly from the interaction of high energy protons and helium with the galactic interstellar medium. The energy spectrum of these components carries fundamental information regarding the propagation of cosmic rays in the galaxy which are competitive with those obtained from other secondary to primary measurements such as B/C. The PAMELA experiment has been observing galactic cosmic rays since July 2006 at an altitude ranging from $\sim$ 350 km to $\sim$ 600 km on-board of the Russian Resurs-DK1 satellite which executes a quasi-polar orbit (70° inclination). The results presented here are based on the data set collected by PAMELA between from July 2006 and December 2007 for the hydrogen and helium isotopes, and between July 2006 and September 2014 for the lithium and beryllium isotopes.

2. The PAMELA instrument

The PAMELA apparatus is composed of several sub-detectors: ToF system, anti-coincidence system (CARD, CAS, CAT), magnetic spectrometer with microstrip silicon tracking system, W/Si electromagnetic imaging calorimeter, shower-tail-catcher scintillator (S4) and neutron detector. A detailed description of the PAMELA instrument and an overview of the mission can be found in [19]. The core of the instrument is a magnetic spectrometer, made of a permanent magnet (0.43 T) and a silicon tracking system (resolution in the bending side 4 μm) for a maximum detectable rigidity of 1 TV. The momentum resolution is better than 4% between 2 GV and 20 GV. The Time of Flight (ToF) system is divided in 6 layers, arranged in three planes, each plane composed of two layers. The first plane (S1) is placed on top of the instrument, the second and third plane are placed above (S2) and below (S3) the spectrometer. The W/Si sampling imaging calorimeter comprises 44 single-sided silicon strip detector planes interleaved with 22 plates of tungsten absorber. Each tungsten layer has a thickness of 0.74 radiation lengths (2.6 mm) and it is sandwiched between two printed circuit boards, which house the silicon detectors as well as the frontend and digitizing electronics. Each silicon plane consists of 3x3, 380 μm thick, 8x8 cm^2 detectors, segmented into 32 strips with a pitch of 2.4 mm. The orientation of the strips for two consecutive silicon planes is shifted by 90 degrees, thus providing 2-dimensional spatial information. The total depth of the calorimeter is 16.3 radiation lengths and 0.6 nuclear interaction lengths.

3. Data analysis

3.1. Event selection

Requirements were set on the event quality to select positively charged particles with a precise measurement of the absolute value of the particle rigidity and velocity. The particle charge for hydrogen and helium particles was identified using the ionization measurements provided by the

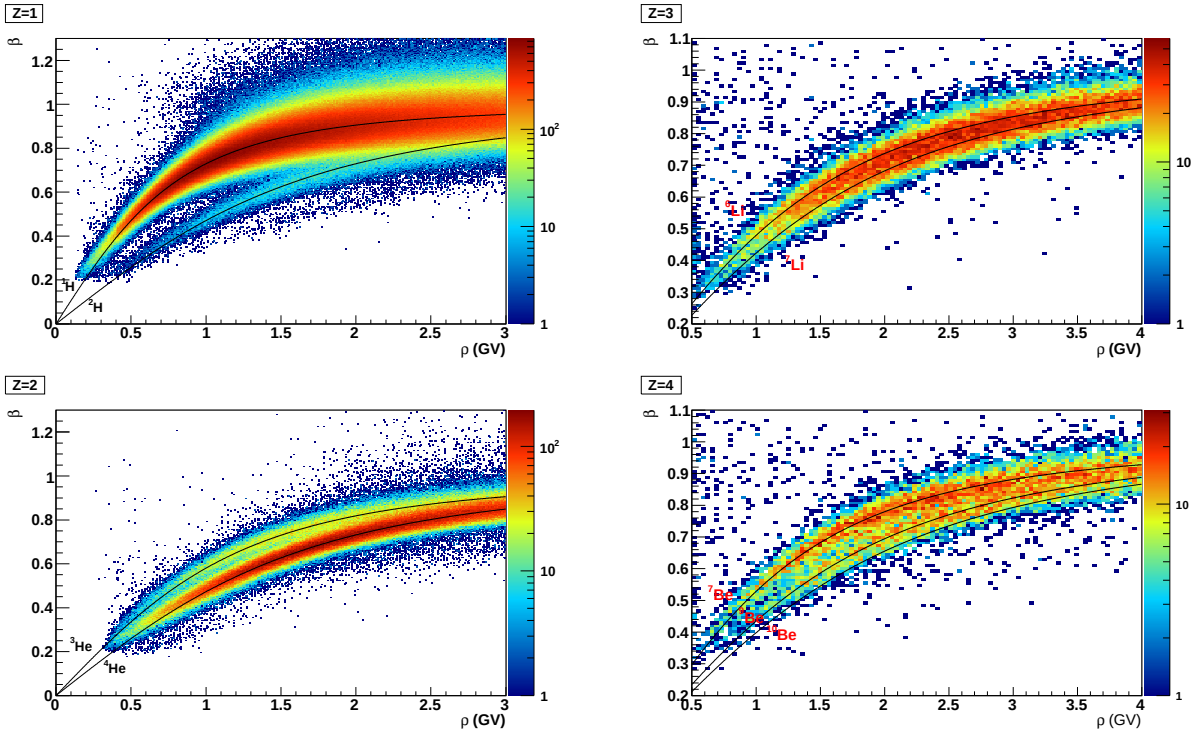

Figure 1. β vs. rigidity for $Z = 1$ (top left), $Z = 2$ (bottom left), $Z = 3$ (top right) and $Z = 4$ (bottom right) particles.

silicon sensors of the magnetic spectrometer. The requirements are identical to the selection in [1] and we refer to this paper for more details. Lithium and beryllium events have been selected by means of ionization energy losses in the ToF system. Charge consistency has been required between S12 and $\langle$S2$\rangle$ and $\langle$S3$\rangle$ (the arithmetic mean of the ionizations for the two layers constituting S2 and S3, respectively).

3.2. Isotope separation in the PAMELA instrument

In each sample an isotopic separation at fixed rigidity is possible since the mass of each particle follows the relation $m = RZe/\gamma\beta c$, where R is the magnetic rigidity, $Z \times e$ is the particle charge, and γ is the Lorentz factor. The particle velocity β can either be provided directly from the timing measurement of the ToF system, or indirectly from the energy loss in the calorimeter, which follows β via the Bethe-Bloch formula $dE/dx \propto \frac{Z^2}{\beta^2}$ (neglecting logarithmic terms). In figure 1 we show β as derived by the ToF system vs. the particle rigidity for the four different charge samples. The black lines in the figure represent the expectations for each isotope.

The isotopic analysis of nuclei with the calorimeter is restricted to events which do not interact inside the calorimeter, selecting events by applying cuts on the ratio between the energy deposited in the strip closest to the track and the neighboring strip on each side and the total energy detected. In a single silicon layer, the energy loss distributions shows a Landau tail which degrades the resolution of the dE/dx measurement. Using a truncation method, the 50% of samples with larger pulse amplitudes are excluded before taking the mean of the dE/dx measurements, thus reducing the effect of the Landau tail. The mean dE/dx for each event vs. the rigidity measured with the magnetic spectrometer for the four different charge samples is shown in figure 2.

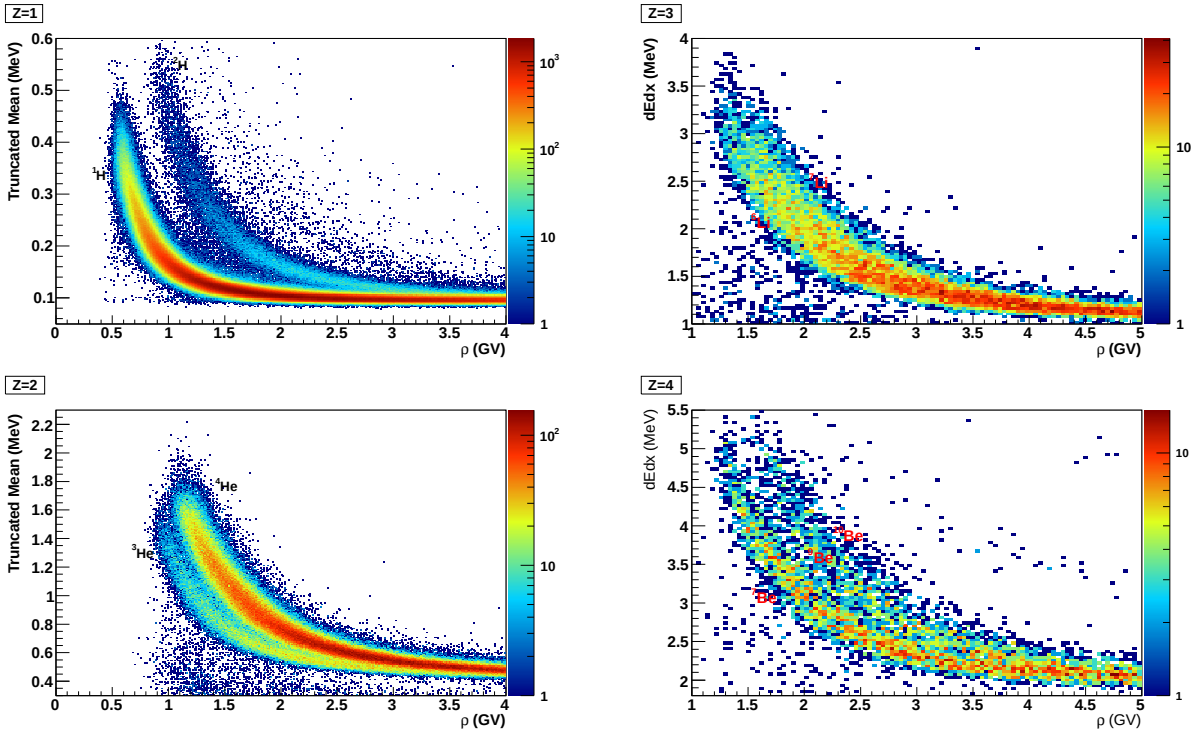

Figure 2. Mass separation for for $Z = 1$ (top left), $Z = 2$ (bottom left), $Z = 3$ (top right) and $Z = 4$ (bottom right) particles using the "truncated mean"-method.

3.3. Raw isotope numbers

For $Z = 1$ and $Z = 2$ particles the counts in each rigidity range were derived in a similar manner as in [1] by fitting gaussians to the $1/\beta$ distributions. $1/\beta$ distributions were chosen since the shape of a $1/\beta$ distribution is gaussian. The dE/dx distributions of the calorimeter have a non-gaussian shape, therefore one has to model the expected distributions of the observable quantities and then perform likelihood fits. The expected dE/dx distributions for each isotope are created using the full Monte Carlo simulation of the PAMELA apparatus based on the `GEANT4` code, which has been already described in [1]. For more details see [15], [16]. For the ToF analysis of $Z = 3$ and $Z = 4$ particles we chose a slightly different approach and created $1/\beta$ distributions using the simulation, and then performed the Likelihood analysis. As an example we show in figure 3 the distributions for ToF and calorimeter for $Z = 4$ in the 1.9 - 2.1 GV rigidity range.

3.4. Flux Determination

To derive each isotope flux the number of selected events derived in the previous section had to be corrected for the selections efficiencies, particle losses, contamination and energy losses. For $Z = 1$ and $Z = 2$ particles most of the corrections could be directly taken from [1]. The analysis of $Z = 3$ and $Z = 4$ particles is in an earlier state, so only isotopic ratios and no fluxes are presented. The efficiency for the calorimeter is derived using simulated data for higher energies and flight data for lower energies, using the redundant detectors to select the isotopes.

4. Results and discussion

In figure 5 and 6 we show the hydrogen and helium isotope fluxes (top) and the ratios of the fluxes (bottom) measured with the ToF or the calorimeter, compared to previous measurements.

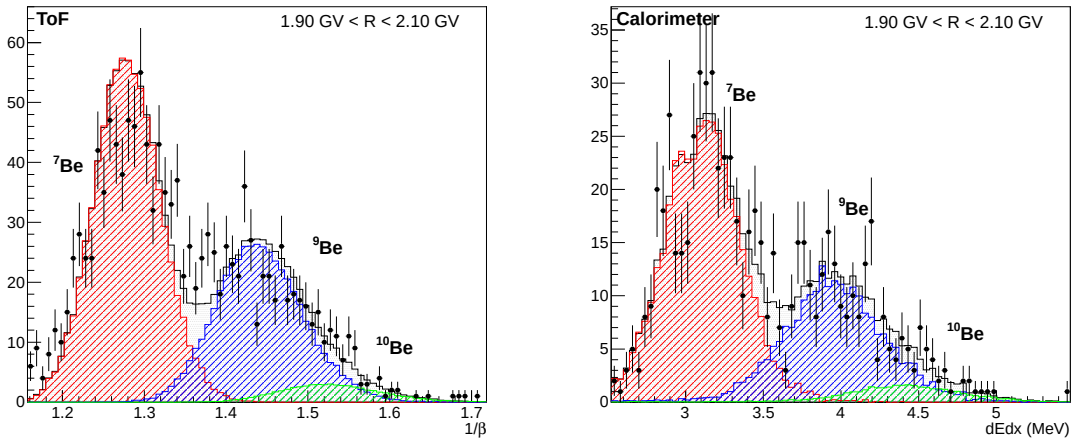

Figure 3. $1/\beta$ distributions of the ToF (left) and truncated mean dE/dx of the calorimeter (right) for beryllium in the 1.9 - 2.1 GV range.

In this context it is important to know that all the former measurements shown in figures 5 and 6, except AMS-01, are from balloon-borne experiments and thus effected by the non-negligible background of atmospheric secondary particle production.

In figure 4 we show some preliminary results for the ratios ^{7}Li/ ^{6}Li and ^{7}Be/(^{9}Be+^{10}Be) derived with the ToF (blue circles) or the calorimeter (red circles) together with other measurements.

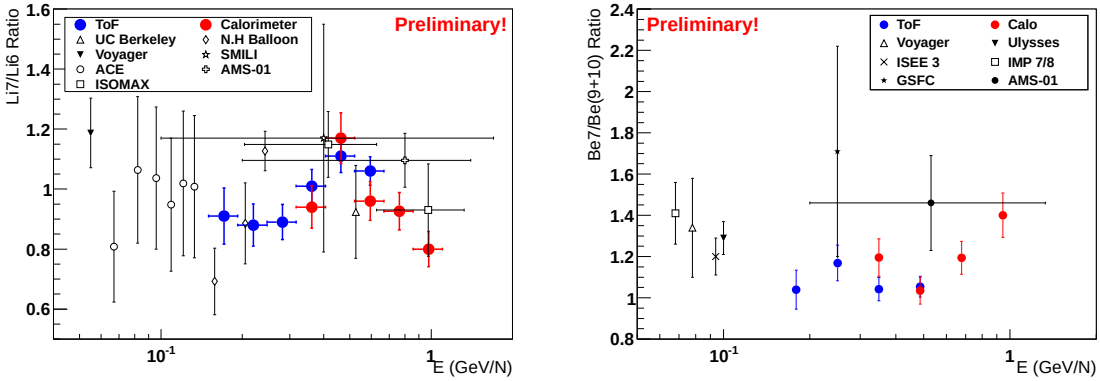

Figure 4. Results for the ratios ^{7}Li/ ^{6}Li and ^{7}Be/(^{9}Be+^{10}Be) derived with the ToF (blue circles) or the calorimeter (red circles). Error bars show statistical uncertainty only. Previous experiments: AMS-01 [4], CRIS/ACE [10], ISOMAX [13], SMILI [5], Voyager [24], UC Berkeley [7], N. H. Balloon [22], Ulysses [8], ISEE-3 [26], IMP 7/8 [11], GSFC [12].

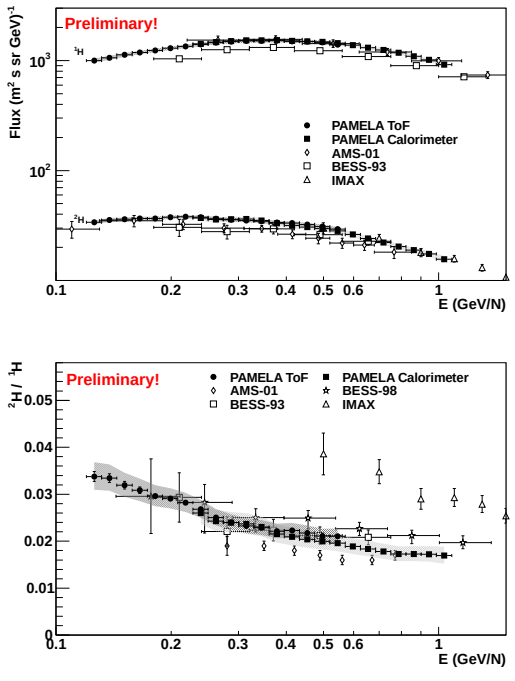

Figure 5. ^{1}H and ^{2}H absolute fluxes (top) and their ratio (bottom) derived with the ToF (circles) or the calorimeter (squares). Previous experiments: AMS-01 [3, 4, 14], BESS-93 [21], BESS-98 [18], IMAX [9]. Error bars show the statistical uncertainty while shaded areas show the systematic uncertainty.

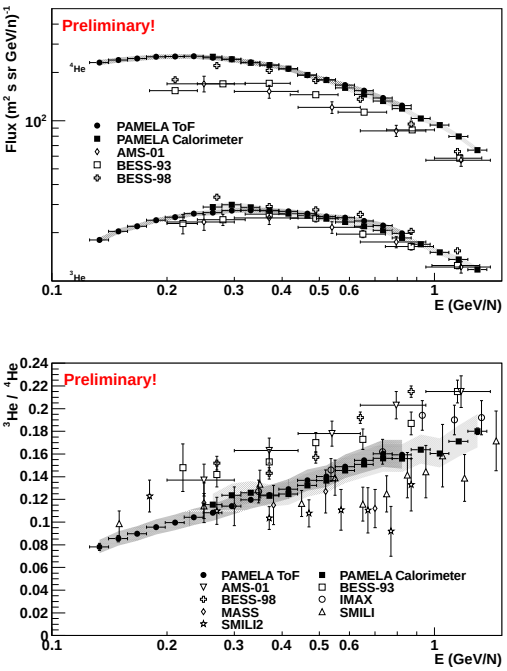

Figure 6. ^{4}He and ^{3}He absolute fluxes (top) and their ratio (bottom) derived with the ToF (circles) or the calorimeter (squares). Previous experiments: AMS [4], BESS-93 [21], BESS-98 [17], IMAX [20], SMILI-1 [6], SMILI-2[25], MASS [23].

References

[1] Adriani O *et al* 2013 *Astrophys. J.* **770** 2
[2] Adriani O *et al* 2014 *Astrophys. J.* **791** 30
[3] Aguilar M, Alcaraz J *et al* 2002 *Phys. Rep.* **366** 331
[4] Aguilar M *et al* 2011 *Astrophys. J.* **736** 105
[5] Ahlen S P *et al* 2000 *Astrophys. J.* **534** 757
[6] Beatty J J *et al* 1993 *Astrophys. J.* **413** 268
[7] Buffington A, Orth C D and Mast T S 1978 *Astrophys. J.* **226** 355
[8] Connell J J 1998 *Astrophys. J.* **501** L59
[9] de Nolfo G A *et al* 2000 *AIP Conf. Proc.* **528** 425
[10] de Nolfo G A *et al* 2006 *Adv. Space Res.* **38** 155864
[11] Garcia-Munoz M, Mason G M and Simpson J A 1977 *Astrophys. J* **217** 859
[12] Hagen F A, Fisher A J, and Ormes J F 1977 *Astrophys. J.* **212** 262
[13] Hams T *et al* 2004 *Astrophys. J.* **611** 892-905
[14] Lamanna G *et al* 2001 *Proc. 27th Int. Cosmic Ray Conf. (Hamburg)* 1617
[15] Menn W *et al* 2013a *J. Phys.: Conf. Ser.* **409** 012030
[16] Menn W *et al* 2013 *Proc. 33nd Int. Cosmic Ray Conf. (Rio de Janeiro)* 0233
[17] Myers Z D *et al* 2001 *Proc. 27th Int. Cosmic Ray Conf. (Hamburg)* 1805
[18] Myers Z D *et al* 2005 *Adv. Space Res.* **35** 151-5
[19] Picozza P *et al* 2007 *Astropart. Phys.* **27** 296
[20] Reimer O *et al* 1998 *Astrophys. J.* **496** 490
[21] Wang J Z, Seo E S *et al* 2002 *Astrophys. J.* **564** 244
[22] Webber W R and Kish J 1979 *Proc. 16th Int. Cosmic Ray Conf. (Kyoto)* **1** 389

[23] Webber W R *et al* 1991 *Astrophys. J.* **380** 230
[24] Webber W R, Lukasiak A and McDonald F B 2002 *Astrophys. J.* **568** 210-5
[25] Wefel J P *et al* 1995 *Proc. 24th Int. Cosmic Ray Conf. (Rome)* **2** 630
[26] Wiedenbeck M E and Greiner D E 1980 *Astrophys. J.* **239** L139